Vacuum Surface Flashover: Experiments and Simulations

J. Z. Gleizer, Ya. E. Krasik
Technion
Physics Department
Haifa 3200, Israel

U. Dai
MoD/DDR&D
Tel-Aviv 61909, Israel

and **J. G. Leopold**
Rafael Laboratories
Department of Applied Physics
POBox 2250, Haifa 31021, Israel

ABSTRACT

It is conjectured that vacuum dielectric surface flashover can be avoided by preventing its initiation. Assuming that the flashover process is initiated by the impact of charged particles on the insulator surface, by deflecting these away from the surface, the development of a flashover avalanche can be repressed. As evidence of this, we present the results of experiments where high-voltage fast-rising microsecond timescale voltage pulses are applied on vacuum insulator samples where we methodically manipulate the magnitude and the orientation of the electric fields at the cathode and anode triple junctions and along the insulator surface.

Index Terms - **Surface flashover, vacuum, dielectric, triple junction, high-voltage.**

1 INTRODUCTION

ONE of the most crucial elements of high-voltage (HV) pulsed power generators and charged particle accelerators that limits the operation and reproducibility is their interface insulators. Vacuum surface flashover along these insulators is accompanied by the formation of plasma, leading to the abrupt termination of an HV pulse applied to the load. Research on insulator surface flashover, in which its mechanism was investigated and the best insulator material or design was sought, has continued for more than 50 years and several review papers [1] and textbook chapters [2,3] related to this subject have been published.

It is thought that vacuum flashover originates from micro-protrusions on imperfectly smoothed conducting surfaces or protrusions formed by cathode spots, which explode to produce plasma from which primary charged particles are accelerated by the high electric fields. Conducting dust particles on insulator surfaces may act similarly. The mechanism for the development of vacuum surface flashover [1] is based on these primary charged particles impacting the insulator surface, leading to the emission of secondary electrons, appearance of a positively charged surface of the insulator at those locations, desorption and ionization of neutrals from the gaseous mono-layers that always exist at the surface of the insulator, and, accordingly, formation of flashover plasma. Recurring insulator surface flashover events result in material damage which ultimately leads to complete insulator breakdown.

It is commonly accepted that elevated voltage gradients across insulator surfaces are the main factor influencing vacuum surface flashover. To reduce flashover probability, HV vacuum systems are often designed with large inter-electrode gaps requiring large insulators to reduce the electric fields responsible for the emission and acceleration of the charged particles participating in the surface flashover avalanche [4]. There is, however, a limit as to the extent to which HV vacuum systems can be degassed, cleaned, smoothed, or designed such that they have reduced electric fields along the insulator surface.

It is also accepted that the triple junctions of the conductor-insulator-vacuum surfaces are likely to initiate flashover. In practice, one always obtains micron-size gaps between the insulator and the conductor. Let us consider these micro-gaps near each triple junction. One can interpret this situation as a simple electrical scheme composed of two capacitors (“vacuum” and “insulator”) connected in series. Then, the electric field in the vacuum capacitor $E_v = \varepsilon\overline{E}$ increases by a factor ε relative to the mean electric field $\overline{E} = \varphi/d$. ε is the dielectric constant of the insulator material, d is the distance between the anode and cathode electrodes and φ is the applied potential difference. This increase in the electric field is caused by the induced insulator surface polarization charges. For the case of an inclined insulator

Manuscript received on 2 March 2014, in final form 14 April 2014, accepted 14 April 2014.

DOI 10.1109/TDEI.2014.004628

where, say, β_C=45° ($\alpha_C = \alpha_A$ = 180°) (see Figure 1), the dielectric is thin near the cathode triple junction (CTJ), which causes the electric field to decrease. In contrast, at the anode triple junction (ATJ), as β_A approaches 135°, the insulator is thick and the electric field increases by the factor ε.

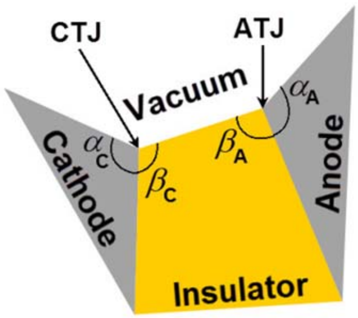

Figure 1. The definition of the orientation angles [5] of the various material surfaces in a *z*-directionally symmetric plane for a situation where an insulator separates a cathode from an anode in vacuum.

This qualitative explanation is supported by the analytical theory of the electric fields at perfect triple junctions [5-7]. A perfect triple junction is a line or a point, which in practice never occurs because of the limits imposed by mechanical tolerances [8]. According to the theory of Chung *et al.* [5], the electric field at a perfect triple junction is given analytically as , where *r* is the distance from the triple junction and *v* depends on the orientation angles of the three connected regions and the dielectric constant of the insulator material (see Figure 1). The theory is exact within a finite small region near the triple junction at $r = 0$, and *A* depends on the applied voltage. Using the theory of Chung *et al.* [5], one can calculate the value of the electric fields at both the CTJ and ATJ. When a cylindrical insulator is placed perpendicularly ($\beta_C = \beta_A$ = 90°, $\alpha_C = \alpha_A$ = 180°) between two flat and parallel electrodes making up a voltage gap in vacuum, $v = 1$ and the electric field at the CTJ and the ATJ is constant and the same as along the length of the entire insulator. At a perfect CTJ of an inclined insulator surface between parallel cathode-anode surfaces ($\beta_C + \beta_A$ = 180°, $\alpha_C = \alpha_A$ = 180°), $v > 1$ (see Figure 6 in Reference 5) and the electric field approaches zero ($r \rightarrow 0$). As the inclination angle β_C at the CTJ decreases below 90° toward 45° the value of *v* increases and as $r \rightarrow 0$ the electric field approaches zero faster. At the same time, at the ATJ the value of *v* decreases below 1 as the value of β_A above 90° increases toward 135° and the electric field approaches infinity at a higher rate as $r \rightarrow 0$. This lead to the suggestion that it is anode-initiated surface flashover [9] that limits voltage holdoff of a β_C = 45° and β_A = 135° inclined insulator.

Extensive experiments on the dependence of the flashover voltage of insulators in vacuum on surface orientation angles were performed by Milton [10]. The results of these experiments supported those of earlier works [4], [11] and suggested that an inclined insulator considerably increases the flashover voltage. These results led to the practice, which is now common in vacuum insulation, of using insulators inclined to (β_C, β_A) = (45°, 135°) between two parallel conducting planes (α_C, α_A) = (180°, 180°). We designate this inclined insulator as β_C = 45°. Milton's results also showed that the flashover voltage increases for fast rising pulses. This can be qualitatively explained by a larger value of the displacement current being required to distribute potential along the insulator surface. The choice of insulator material [2, 10] and the HV pulse duration [10, 12-13] have also been found to be important. A decrease in the duration of the HV pulse from a microsecond time scale to tens of nanoseconds leads to a significant (up to factor 2) increase in the value of the flashover voltage [2]. These empirically obtained data strongly indicate that several phenomena are involved in the initiation and evolution of surface flashover. For instance, one can consider two competitive processes that determine the potential gradients at insulator surface imperfections. If the flashover is initiated at imperfections, there will be a potential gradient increase due to the electron emission being proportional to the product of the current intensity of the emission and time. However, due to finite surface resistivity, which is material-dependent and depending on the vacuum level and the level of surface cleanliness, the elementary discharge of stray capacitance will contribute to a decrease in the potential gradient.

The highest experimental flashover fields achieved were for a β_C = 45° inclined insulator. Over the years, attempts were made to reach even higher flashover fields. Stygar *et al.* [9] reconfirmed earlier results (see references quoted in Ref. [9]) and observed a dramatic increase in the flashover field, by a factor of ~1.5 relative to the β_C = 45° case, when conducting *plugs* are applied near the ATJ. These experiments displayed the highest vacuum insulator flashover field limits ever obtained. It was shown that the chosen anode plugs reduce the electric fields at and close to the ATJ, to which Stygar et al relate the increase in the flashover voltage. Thus, one of the main conclusions of their research was that the Anderson model [9] for anode-initiated flashover is relevant. This model suggests that the extreme anode end electric fields cause the emission of dielectric surface electrons, which in turn cause the development of a sub-surface dielectric breakdown branching toward the cathode, causing catastrophic bulk burnout of the insulator.

We have suggested that, by controlling the orientation of the electric and magnetic fields and the electro-magnetic fields in a time-dependent HV vacuum system, so that charged particles are deflected from impacting the insulator surface, flashover properties can be considerably improved even if electric fields are not reduced [8]. This conjecture has been experimentally demonstrated [14-15] but not systematically studied until now.

In this paper, we report the experimental results of vacuum surface flashover for dielectric samples under the effect of fast rising (~50 ns) several microsecond-long HV pulses. We apply conducting inserts and protrusions near the triple junctions to control the orientation of the electric fields. We simulate [16] by calculating electron trajectories and the electric field orientation to show that, when primary electrons are deflected from the cathode triple junction and from most of the insulator surface, the flashover voltage improves significantly. We also show that, when the electric field approaches infinity at the ATJ, flashover is not necessarily initiated there. We have not found experimental evidence that when the electric field at the ATJ is considerably reduced flashover is prevented.

2 EXPERIMENTAL SETUP AND METHODS

Our experimental setup is shown in Figure 2. A 6-stage transformer oil-filled bi-polar charged Marx generator (maximal charging voltage φ_{ch} = ±50 kV, output capacitance C_M ≈ 1.7 nF) having three Maxwell gaseous spark gap switches with a middle field-distortion electrode was used to supply an HV pulse through an interface HV insulator to the anode electrode. Due to resonance, the amplitude of the voltage pulse reaches 330 kV at φ_{ch} = ±40 kV with a rise time of ~50 ns. In order to limit the duration of the HV pulse when flashover did not occur in the tested sample, a resistive load of R_L = 5 kΩ was placed in the transformer oil-filled tank in parallel to the anode-cathode gap, resulting in a time decay of the HV pulse of τ ≈ 10.5 μs. To trigger the Marx generator, an HV pulse of ~40 kV amplitude and ~10 ns rise-time produced by a spiral generator charged to ~3 kV was applied to the middle electrode of the Marx generator spark switches. The waveform of the Marx generator output HV pulse was measured using a resistive voltage divider placed at the input of the interface insulator in the oil-filled tank and the discharge current was measured using a self-integrated Rogowski coil (Figure 2).

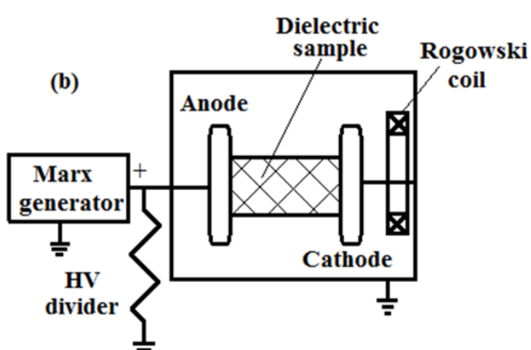

Figure 2. The experimental setup at the Technion (a) and the sample arrangement in the vacuum chamber (b).

Experiments were conducted in a stainless steel vacuum chamber (Figure 2) 400 mm in diameter and 500 mm in length. A turbo-molecular pump was used to produce ~1 mPa background pressure in the chamber. The anode and cathode electrodes were 130 mm in diameter with rounded (r = 5 mm) edges made of polished stainless steel cleaned of organic residues with Ethanol. Dielectric samples of width d were placed between these electrodes.

A conditioning process was applied in each set of experiments using dielectric samples of 50 mm diameter made of ULTEM (ULTEM is the commercial name of unfilled Ployetherimide (PEI) known to have high dielectric strength). Namely, the amplitude of the HV pulse applied to the sample placed between the electrodes was gradually increased to its maximal amplitude at which the flashover phenomenon was obtained. Conditioning is known to clean conducting surfaces partially by allowing the micro-protrusions and gas residues to clear while contributing only small pre-flashover currents without causing damage to the insulator. Without conditioning, the explosion of micro-protrusions may end in catastrophic flashover not necessarily typical to insulator surface flashover. Each series of the conditioning experiments was started with a low Marx generator charging voltage of ~12 kV. Then, the charging voltage of the Marx generator was increased in steps of 1.5-2 kV (equivalent to 10-15 kV steps in the cathode-anode gap voltage). Typically, ~100 shots were applied for each voltage step. If no flashover occurred, or only very few (≤5 out of 100), the applied voltage was increased until the sample no longer sustained the voltage. Prior to testing a new sample, the electrodes were re-polished and cleaned and conditioning was restarted. Typical waveforms of the voltage and current obtained in open-circuit and short-circuit experiments are presented in Figures 3 and 4.

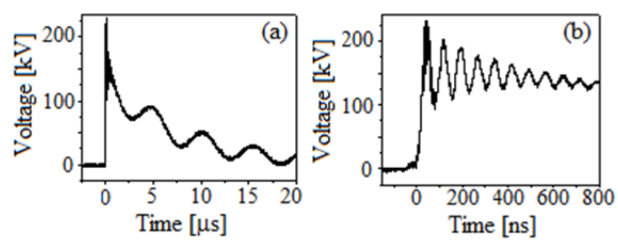

Figure 3. The voltage waveform of an open-circuit experiment with 35 kV charging voltage. In (b), the first 800 ns of the HV pulse in (a) is shown.

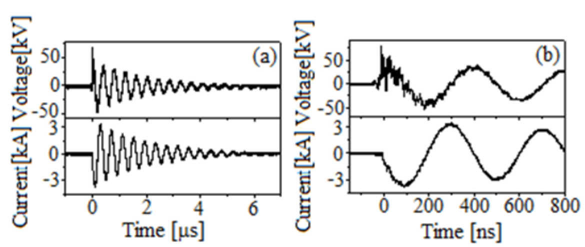

Figure 4. Voltage and current waveforms of a short-circuit experiment with 35 kV charging voltage. In (b) the first 800 ns of the waveforms in (a) are shown.

The internal resistance and inductance of the generator with a short-circuit load obtained from the short-circuit experiment is ~1 Ω and 0.6 μH, respectively. The high-frequency (~5 MHz) oscillations of the voltage waveform obtained in the open-circuit mode of the Marx generator operation are related to the resonance frequency of the Marx generator. Typical flashover waveforms of the applied voltage and discharge current in the case of surface flashover for a d = 10 mm cylindrical ULTEM sample are shown in Figure 5. In these experiments, the time delay between the appearance of the discharge current and the rise of the HV pulse was in the range 30 – 200 ns.

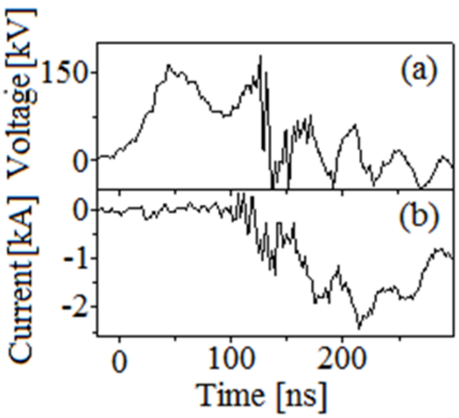

Figure 5. Waveforms of discharge voltage (a) and current (b) for the case of 10 mm in length ULTEM cylindrical sample surface flashover.

When flashover along the dielectric surface occurs, accompanied by formation of surface plasma, the voltage divider showed mainly inductive voltage $\varphi = LdI/dt$ (the resistive voltage drop on the plasma and cathode holders is significantly smaller; L is the anode holder inductance). Note here, that the negative polarity of the current waveform shown in Figures 4b and 5 is in fact positive. The orientation of the Rogowski coil measuring the current determines the polarity of the current waveform. Flashover events of the type seen in Figure 5 occurred during the conditioning process. Apart from surface treeing, these cause no permanent damage to the insulator. In fact, when the voltage is reduced following flashover occurrences, the insulator withheld the voltage.

3 Results and Discussion

Vacuum surface flashover is a complex dynamical process affected by various parameters, the time dependence of the applied voltage included. In order to obtain a baseline for comparisons, experiments on cylindrical insulators between two parallel conducting electrodes were performed. In Figure 6, the conditioning process and the flashover voltage are displayed for inter-electrode gaps d = 10 mm and 15 mm. Here n_p is the number of applied HV pulses for which flashover was not observed. For n (typically 100) applied HV pulses, the number of flashover occurrences (n-n_p) is counted. φ is the maximum of the applied voltage and a mean electric field is defined as = φ/d. When $n_p/n < 0.95$ and not rising again, we define the surface flashover field = E_{fl}. Milton [10] found that with $\beta_C = \beta_A = 90^o$ and 5 μs rise-time pulses most insulators with height d = 12.7 mm experience surface flashover at E_{fl} ~ 35 kV/cm, and with short 50 ns rise-time pulses Lucite experienced flashover at E_{fl} ~ 138 kV/cm [10-11]. In the present experiments, Figure 6 shows that for the waveform seen in Figures 3 and 4 and d = 10 mm, surface flashover for ULTEM occurs at E_{fl} = 185 kV/cm, and when d = 15 mm the value of E_{fl} decreases to 165 kV/cm, which is larger than the values reported in Refs. [10] and [11]. One expects that, for cylindrical insulators, as the length increases, flashover should occur at the same mean electric field, that is, at a higher applied voltage. We see here that flashover does not follow the linearity of the electric field with insulator length.

The results in Figure 7 show the dependence of the flashover field on the inclination angle β_C and $\beta_A = 180^o - \beta_C$ (see Figure 1 for the definition of the angles). Here, the samples were of height d = 10 mm and β_C was either acute (45^o) or obtuse (135^o). The results in Figure 7 confirm that the surface flashover field of a $\beta_C = 45^o$ inclined insulator is superior to that of cylindrical insulators [10-11]. For the voltage waveform used in the present study, for an inclined insulator with $\beta_C = 45^o$, the flashover voltage is ~1.6 times that of a cylindrical insulator, and with $\beta_C = 135^o$ it is ~1.2 times. Thus, these results are consistent with well-known results [10-11].

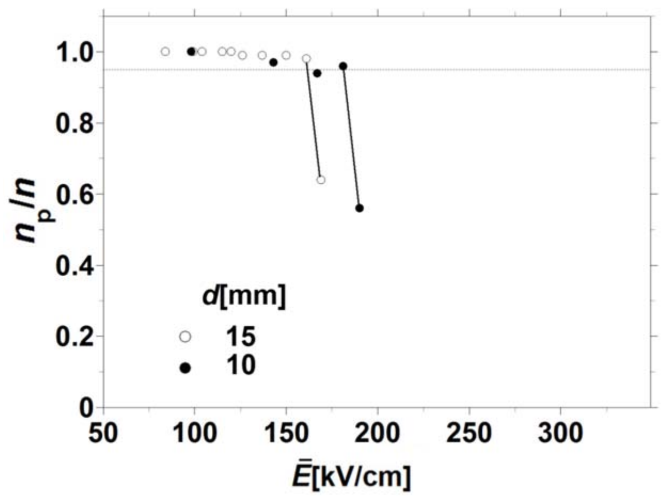

Figure 6. The conditioning and flashover (n_p/n vs.) for two cylindrical insulators of two different heights, d=10 mm and 15 mm. The flashover is defined when n_p/n drops considerably below 0.95. The flashover field E_{fl} is defined as between the two experimental points connected by lines.

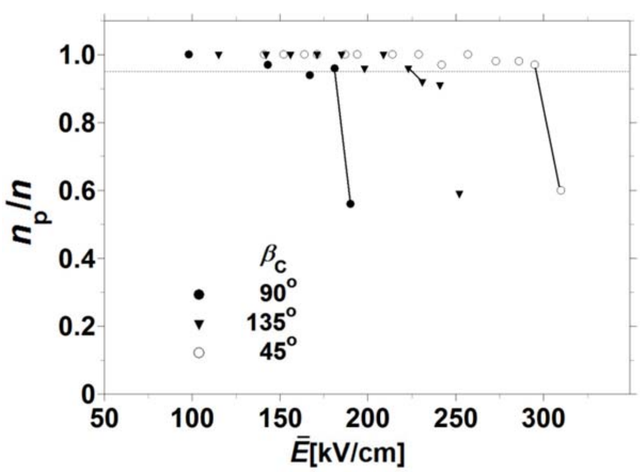

Figure 7. The ratio n_p/n vs. for samples with different inclination angles β_C. The height of all samples was d = 10 mm. The flashover field is indicated by connecting lines as defined.

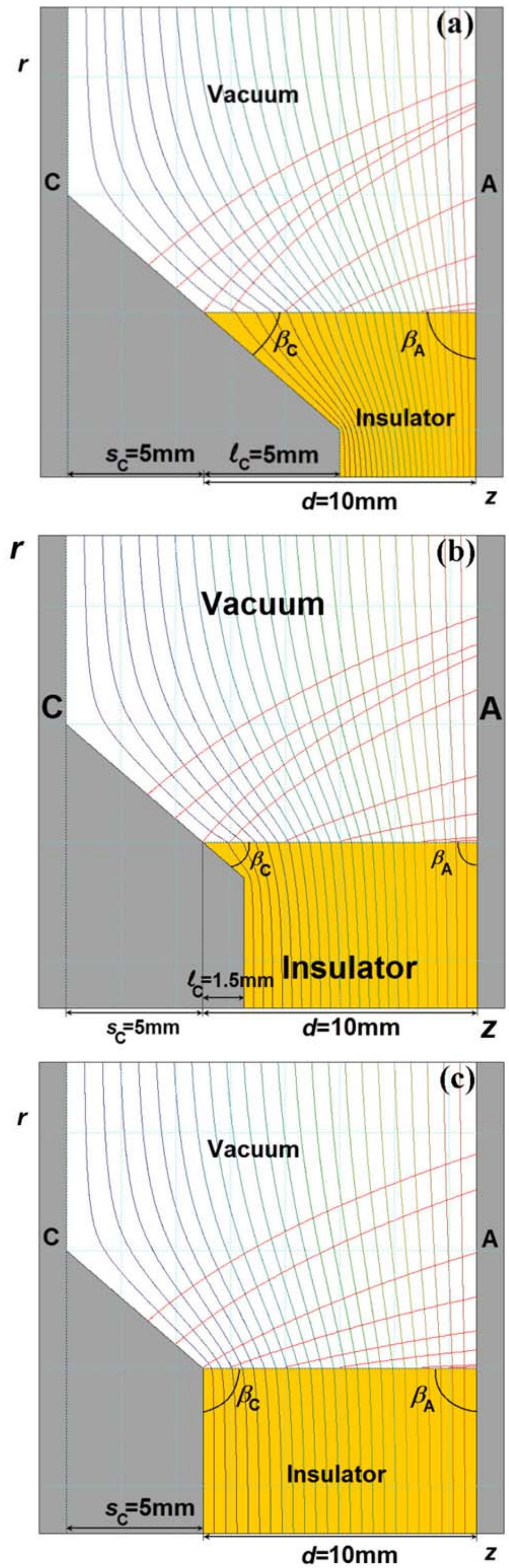

Figure 8. The cylindrical geometry, equi-potential contours and low current electron trajectories (red orbits crossing equi-potential curves) for a cathode insert. d = 10 mm and ε_r = 3.5 for all cases. In (a) ℓ_C = 5 mm, (b) ℓ_C = 1.5 mm and β_C = 45°. In (c) ℓ_C = 0 and β_C = 90°. All such inserts are on top of a 45° inclined step of height s_C = 5 mm. Low current electrons are initiated for all cases at the same initial position and 300 kV is applied.

An explanation [8] for the effect of the inclination angle on the flashover field is that when it is acute, β_C < 90°, the orientation of the electric field along the entire insulator surface is such that electrons, whether primaries emitted from the cathode surface or first generation secondary electrons emitted from the insulator surface by uncontrolled charged particle or UV photons impact, are deflected from the insulator and the probability that an avalanche will develop is reduced. When β_C is obtuse, electrons emitted from the cathode surface may impact the insulator surface, but because the electric field attracts electrons toward the insulator, only a small amount of secondary electrons acquire sufficient energy to be emitted, and therefore, it is more difficult to start an avalanche. When β_C = 90°, electrons started near the CTJ accelerate along trajectories parallel to the insulator surface. Because of surface imperfections and the gas mono-layer, electrons initiated close to the CTJ can graze the insulator surface and a flashover avalanche may develop. As β_C increases, these electrons are increasingly accelerated away from impacting the surface. To test this qualitative explanation, several insulators with different cathode inserts were tested (see Figure 8).

The cathode insert in Figure 8 is composed of a conducting part penetrating the insulator and an oblique step penetrating the vacuum region. When β_C = 45°, the CTJ thus formed has the same topology as that of a 45° inclined insulator (Figures 8a and b). When the height of the penetrating part l_C = 0, the topology of the CTJ changes to β_C = 90° (Figure 8c). β_A = 90° in Figure 8 and the ATJ has the topology of an insulator surface perpendicular to the anode surface. Figure 8 shows that a cathode insert inclines the equi-potential contours and, respectively, causes most electrons to be accelerated away from the insulator surface. As the penetrating part's height, l_C, decreases, electrons emitted on the insulator surface close to the anode graze the insulator surface. The dependence of the experimental flashover electric field on the value of l_C is shown in Figure 9.

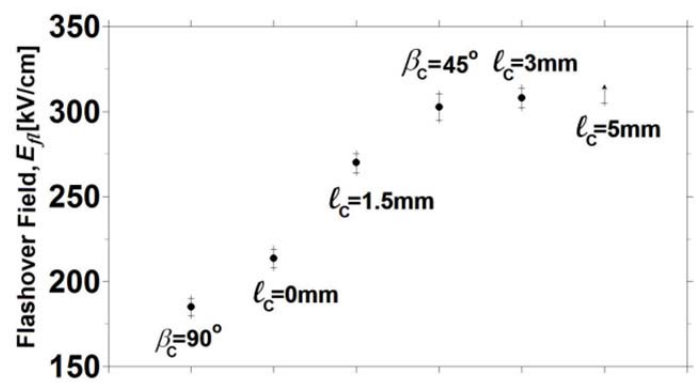

Figure 9. Experimental flashover fields for cathode inserts with ℓ_C = 5 mm, 3 mm, 1.5 mm and 0 mm compared to those obtained for a cylindrical insulator β_C=90°(β_A=90°) and a 45° inclined insulator β_C = 45°(β_A = 135°). For all these cases d = 10 mm and s_C = 5 mm. The experimental value (●) is drawn midway between the value measured at flashover and immediately before flashover occurred. The error in the flashover field measurement is considerably smaller.

Here let us note that for l_C = 5 mm, increasing the amplitude of the HV pulse above 300 kV caused a bulk breakdown of the sample initiated along the cathode insert penetrating the insulator, indicating that the flashover field is >300 kV/cm.

One can see that the application of a step on its own ($l_C = 0$) is sufficient to increase the flashover field above that of a cylindrical insulator. In addition, an insert of l_C = 3 mm is sufficient to cause the surface flashover of the insulator at fields similar to those for an ordinary inclined insulator [β_C = 45° (β_A = 135°), ($\alpha_C = \alpha_A$ = 180°) in Figure 1], and an insert of l_C = 5 mm probably performs even better. These experimental results show that the stronger the electron deflection from the cathode onward toward the anode, the better the voltage holdoff. Moreover, we have been able to reproduce and improve the flashover field of a cylindrical insulator as compared to that of a 45° inclined insulator by manipulating only its CTJ with a cathode insert of height $l_C >$. For a more quantitative comparison, we display in Figure 10 the calculated electrostatic field [16] magnitudes and orientations for the various cases considered in Figure 9.

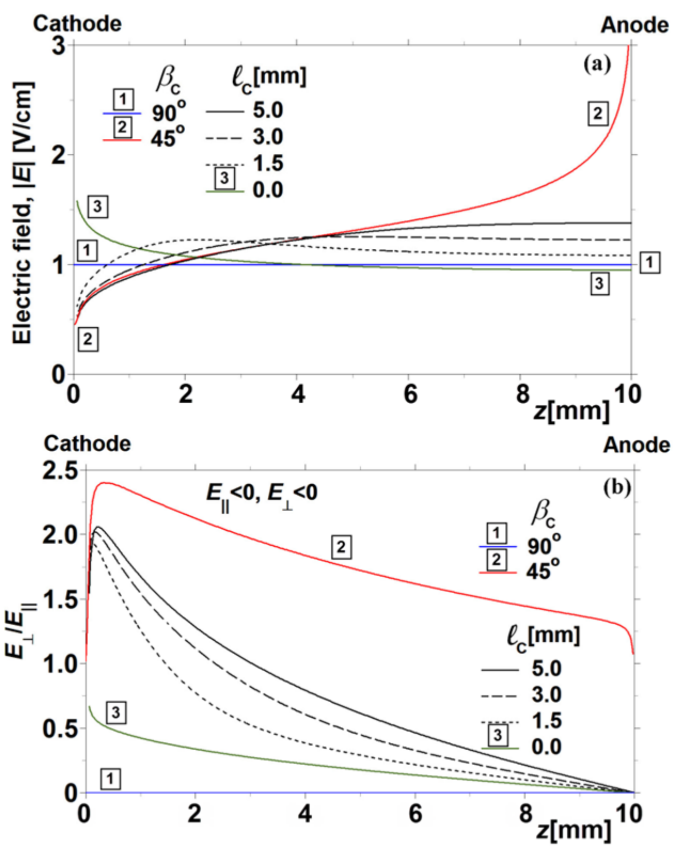

Figure 10. (a) The calculated absolute value of the electric field in vacuum for insulator (ε_r = 3.5) samples between two parallel conducting surfaces along a line parallel to and at a distance of 50 µm from the insulator surface. 1V is applied between the cathode and anode surfaces, which are at z = 0 mm and 10 mm, respectively, along the surface of the d = 10 mm insulator. Various insert penetration depths l_C are considered and compared to calculations of a β_C = 45° (β_A = 135°) (2) inclined insulator and a cylindrical insulator β_C = 90° (β_A = 90°) (1). (b) The inclination of the electric field vector relative to the insulator surface along the same line as in (a). Note that $E_\perp = 0$ for β_C = 90°.

The absolute value of the electric field (Figure 10a) near the CTJ for all cathode inserts with $l_C > 0$ approaches zero at the CTJ because β_C = 45°. With the highest insert considered (l_C = 5 mm) the decrease in the magnitude of the electric field is close to that of a β_C = 45° (β_A = 135°) inclined insulator from ~d/2 and toward the CTJ. As l_C decreases, so does the distance from the CTJ where the field starts to decrease. For $l_C = 0$, the topology of the CTJ changes (β_C = 90°, α_C = 135°) and the magnitude of the electric field increases above that of a cylindrical insulator as the CTJ is approached. As the ATJ is approached, the electric field approaches an infinite value for the inclined insulator (β_A = 135°) and a finite value for all other cases, which approaches the value of the electric field of a cylindrical insulator as l_C decreases. For $l_C = 0$, the electric field as the ATJ is approached becomes somewhat less than that of a cylindrical insulator.

In general, flashover is often related to the magnitude of the electric field (Figure 10a) and it is assumed that a reduction in the electric field reduces its probability. Perhaps the most significant point to notice is that a reduction in the electric field near the ATJ does not cause an increase in the flashover field as compared to an inclined insulator (Figure 9). We also see that the order in which the field magnitude decreases (Figure 10a) along the insulator surface does not follow the order of increase in the experimentally observed flashover fields for the different cases considered.

On the other hand, the dependencies of the ratio of the field components $E_\perp / E_\|$ (Figure 10b) are consistent with the results of the experiment (Figure 9). Here, $E_\perp$ and $E_\|$ are the components of the electric field that are perpendicular and parallel to the insulator surface, respectively, and the ratio $E_\perp / E_\|$ represents the field inclination near the insulator surface. $E_\|$ for all cases considered is negative, indicating that electrons are accelerated from the cathode toward the anode. A positive value of $E_\perp$ signifies that electrons are accelerated away from the insulator surface for all the cases in Figure 10b. The larger the ratio $E_\perp / E_\|$, the larger the electric field inclination angle from the insulator surface. In Figure 10b, one can see that $E_\perp / E_\| \sim 2$ near the CTJ is sufficient for obtaining flashover fields that are the same as or even higher than those of the 45° inclined insulator. As l_C increases, the field orientation, i.e., the ratio $E_\perp/E_\|$, near the CTJ, also increases. On the other hand, as one approaches the ATJ, the field inclination angle decreases to zero at the ATJ. (For an inclined insulator, this is because $|E| \to \infty$, whereas for all other cases $E_\perp \to 0$.) The strong deflection of electrons from the insulator surface near the ATJ for a 45° inclined insulator is probably not a necessary condition for better flashover properties. On the other hand, there seems to be a lower bound to the field inclination angle as the ATJ is approached, below which there is too much electron surface grazing, which contributes to the reduction of the flashover field toward that of a cylindrical insulator.

Next, we manipulate the ATJ using an anode protrusion, as seen in Figure 11, while leaving the CTJ the same as that of a cylindrical insulator.

An anode protrusion with β_A = 135° mimics the ATJ of a 45° inclined insulator. One can see that as the protrusion penetrates the vacuum more deeply it attracts electrons emitted close to the CTJ, which would otherwise graze the insulator surface causing flashover. The more deeply the

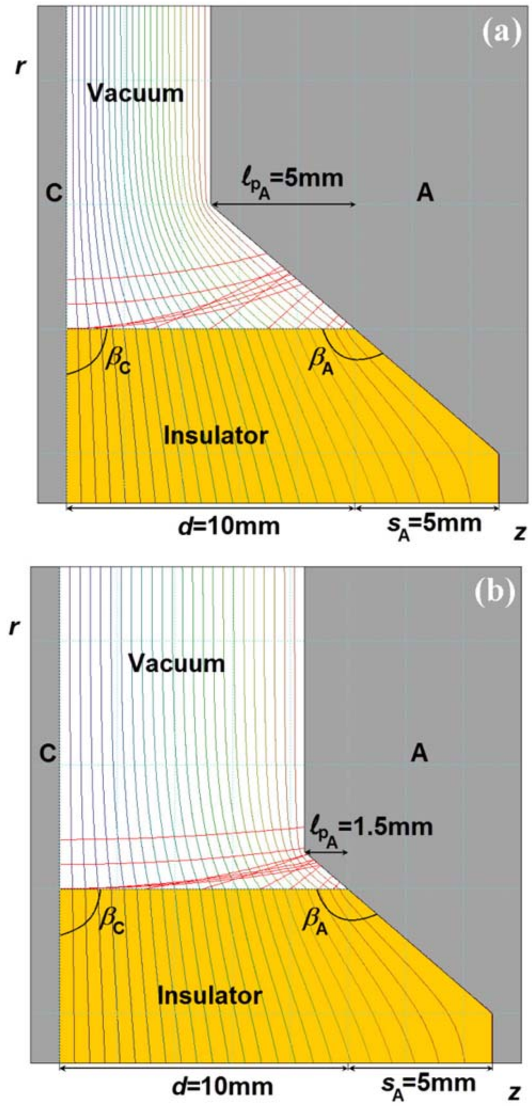

Figure 11. Same as Figure 8 for an anode protrusion with $\beta_A = 135^o$ ($\beta_C = 90^o$) at the end of a fixed anode step s_A = 5 mm. d = 10 mm and the protrusion height is l_{pA} = 5 mm (a) and 1.5 mm (b).

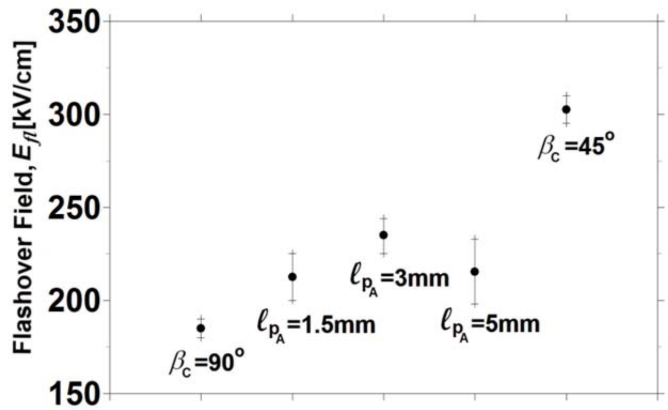

Figure 12. Experimental flashover fields for anode protrusions with l_{pA} = 5 mm, 3 mm, 1.5 mm compared to those obtained for a cylindrical insulator $\beta_C = 90^o$ ($\beta_A = 90^o$) and an inclined insulator $\beta_C = 45^o$ ($\beta_A = 135^o$).

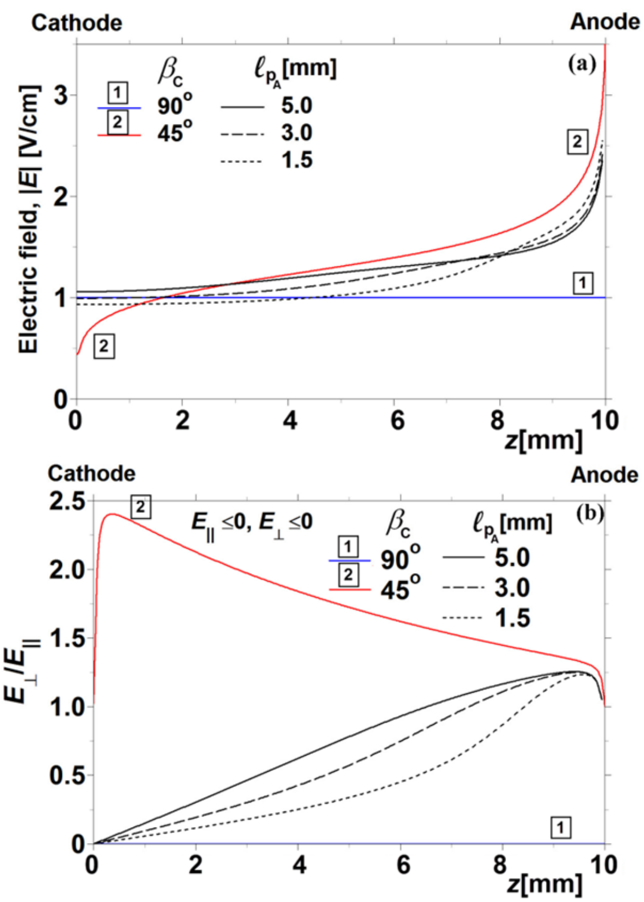

Figure 13. Same as Figure 10 for the geometry of Figure 11.

protrusion penetrates the vacuum, the less surface grazing occurs. In Figure 12, the experimentally measured flashover fields for various anode protrusion heights l_{pA} are displayed. One can see that, even though the electric field at the ATJ theoretically approaches infinity for all protrusions, deflecting the electron trajectories somewhat from grazing the insulator surface is sufficient to improve the flashover fields relative to the cylindrical case. Thus again, it seems that deflecting electrons away from the surface affects the flashover field more than the presence of very high fields at the ATJ.

In Figure 13a, we show the absolute value of the electric field, whereas in Figure 13b we show the field orientation along the insulator surface for various values of l_{pA}.

Figure 13a shows that with an anode protrusion (Figure 11), the approach of infinite electric fields at the ATJ is more moderate and the electric fields nearby are lower than for a 45^o inclined insulator. The electric field at the CTJ is affected only a little as compared to that of a cylindrical insulator. The electric field inclination (Figure 13b) is such that electrons are deflected along the entire surface. Near the CTJ, the field inclination decreases with decreasing l_{pA}, but it is enough to cause an increased flashover field (see Figure 12). Thus again, one can conclude that even a small deflection of the electrons near the CTJ is sufficient reason for the increased flashover fields as compared to a cylindrical insulator, and the very high electric fields at the ATJ do not contribute significantly.

Next, we tested anode inserts of the type seen in Figure 14. The geometry of an anode insert is the mirror image of a cathode insert (see Figure 8).

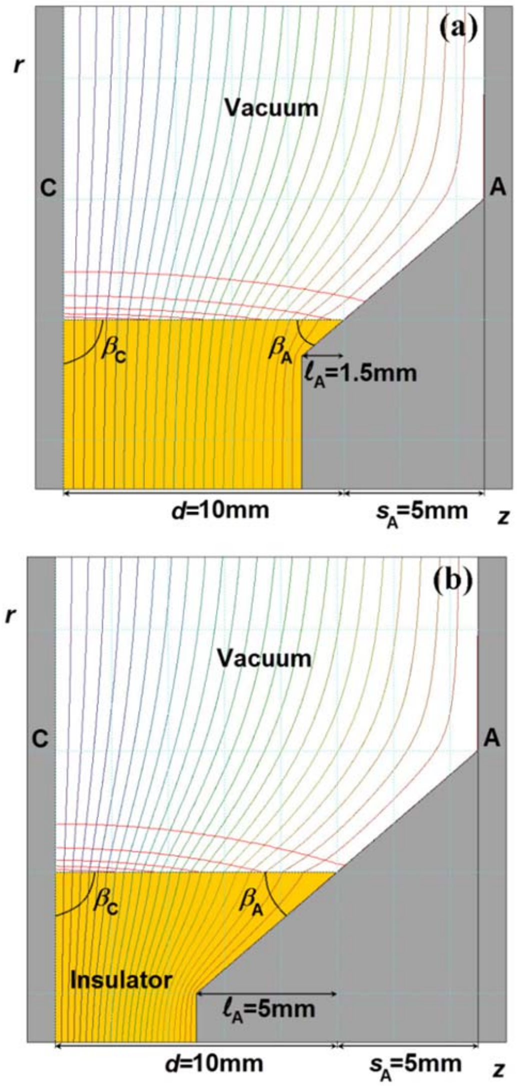

Figure 14. Same as Figure 8 for a geometry with a l_A = 5 mm (a) and 1.5 mm (b) anode inserts and β_A = 45°, β_C = 90°.

One can see that, whereas a cathode insert causes electrons emitted near the cathode to accelerate away from the insulator, an anode insert makes these electrons graze and impact the insulator surface. This is reflected in the experimental results seen in Figure 15. Indeed, the deeper the anode insert penetrates the insulator, a lower flashover field is obtained.

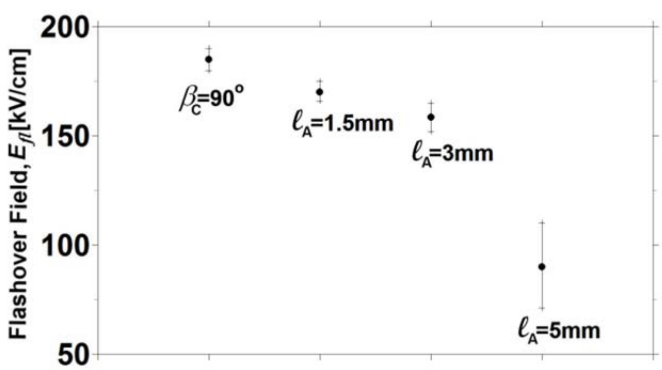

Figure 15. Experimentally measured flashover fields for various anode inserts (Figure 14) with d=10 mm, s_A=5 mm and β_A =45°, β_C=90° as compared to a cylindrical insulator designated as β_C=90°.

An anode insert reduces the electric field at the ATJ as compared to that of a cylindrical insulator and to the very high to infinite fields of a 45° inclined insulator (see Figure 16a). Along the rest of the surface, the electric field increases above that of a cylindrical insulator. The electric field increases at the CTJ with increasing l_A as compared to that of a cylindrical insulator, which is consistent with the experimental results. At the ATJ, however, the electric field approaches zero as compared to that of the cylindrical insulator and infinity for a 45° inclined insulator, in contrast to the experimental results. Thus, the magnitudes of the electric field at the triple junctions or along the insulator surface are not sufficiently consistent to explain the experimental results (Figure 15).

On the other hand, the field inclination for all anode inserts considered (see Figure 16b) is consistent with the strong acceleration of electrons toward the surfaces close to the ATJ and indeed along the entire surface. The latter is consistent with the reduction in the flashover field to less than that of a cylindrical insulator with increasing l_A observed in the experiments (see Figure 15).

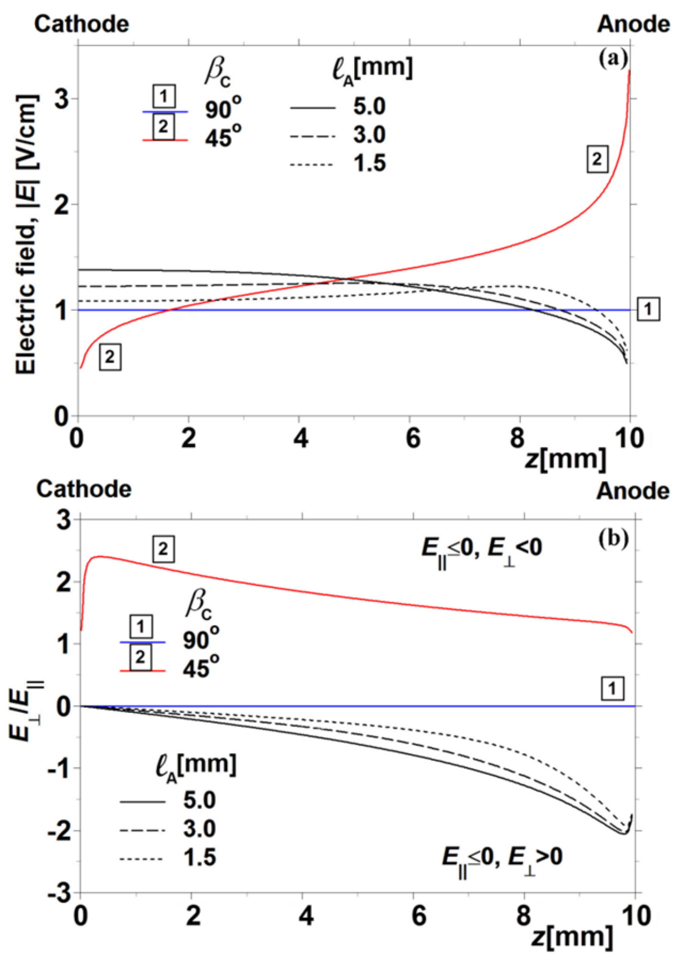

Figure 16. Same as Figure 10 for the geometry of Figure 14.

We have so far tested the effect of manipulating the electric fields near each separate triple junction by using cathode or anode inserts and anode protrusions of 1.5 mm, 3 mm, and 5 mm width, ~d/6.7, ~d/3.3, and d/2 respectively, for d = 10 mm samples. We have seen evidence, consistent with our conjecture [8] that controlling the field orientation so that primary electrons and first generation secondary electrons emitted from the insulator surface are deflected away from the insulator surface even for µs-scale duration voltage pulses seems to be important in order to obtain higher flashover fields. A reduction in the magnitude of the electric field does not necessarily improve voltage holdoff. We have also observed that the flashover field does not scale linearly with d, even for a cylindrical insulator (see Figure 6).

We have also measured the flashover field for a cylindrical insulator with both a cathode and an anode insert with $l_C = l_A = 1.5$ mm (Figure 17).

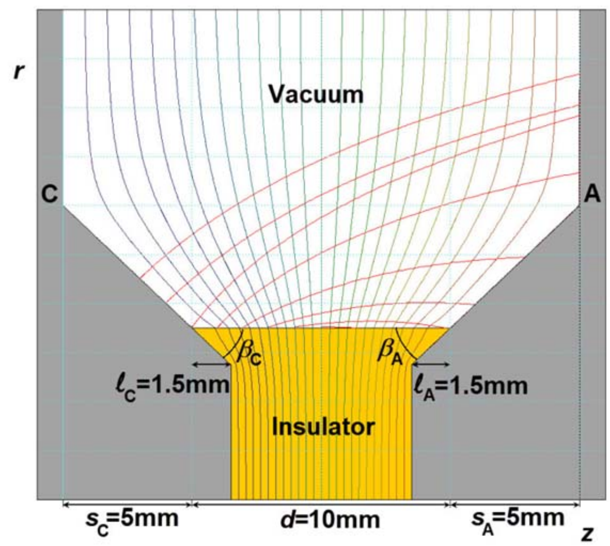

Figure 17. Same as Figure 8 for the geometry including a cathode and an anode insert of $l_C = l_A = 1.5$ mm over a cathode and anode step of $s_C = s_A = 5$ mm and $\beta_C = \beta_A = 45^o$.

For this arrangement, the cathode insert accelerates the primary and first generation of secondary electrons away from the insulator, mimicking the CTJ of a 45^o inclined insulator, but the effect of this insert is countered by the anode insert, which causes some of the electrons to graze or impact the insulator surface. This is reflected in the experimental results seen in Figure 18. The flashover field for this example lies below that of a sample with only a cathode insert of the same depth but above that of a cylindrical insulator, which means that most flashover initiating electrons originate at the cathode end and within the cathode half of the insulator and that the anode insert attracts some of these toward the insulator surface to make the flashover field lower than that of $l_C = 1.5$ mm.

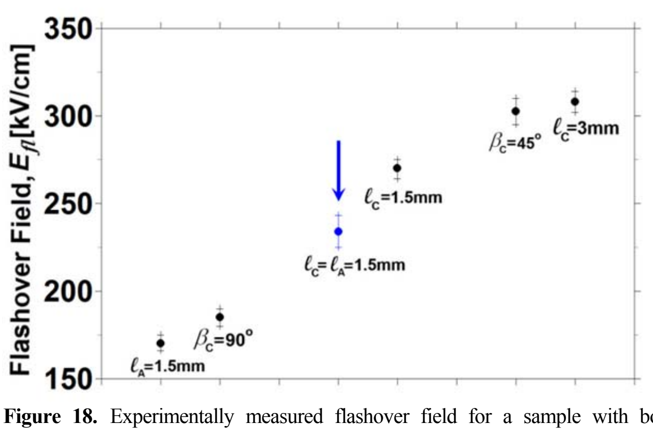

Figure 18. Experimentally measured flashover field for a sample with both cathode and anode inserts $l_C = l_A = 1.5$ mm (Figure 17) ($d = 10$ mm, $s_C = s_A = 5$ mm and $\beta_C = \beta_A = 45^o$ compared to other relevant experiments (Figures 9, 12 and 15).

Finally, we tested a cylindrical insulator sample with an $l_C = 1.5$ mm cathode insert, an anode insert, $l_A = 1.5$ mm, and an anode protrusion, $l_{pA} = 1.5$ mm, shown in Figure 19. The anode insert together with the anode protrusion mimic the ATJ of a 45^o inclined insulator with an applied *anode plug* studied by Stygar *et al*. [9]. Such a Stygar-type ATJ is a $\beta_A = 45^o$, $\alpha_A = 270^o$ triple junction. The electron trajectories in Figure 19 are similar to those seen in Figure 8b. A comparison of the experimentally measured flashover fields for this case and the results obtained for other geometries discussed earlier is shown in Figure 20.

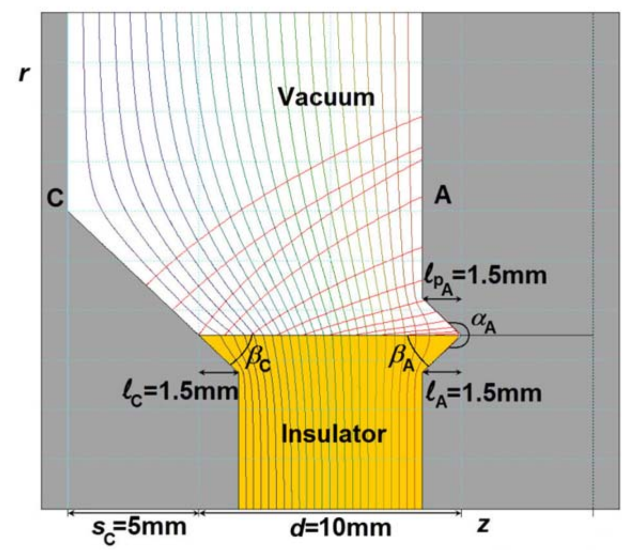

Figure 19. Same as Figure 17 but with an added $l_{pA} = 1.5$ mm anode protrusion.

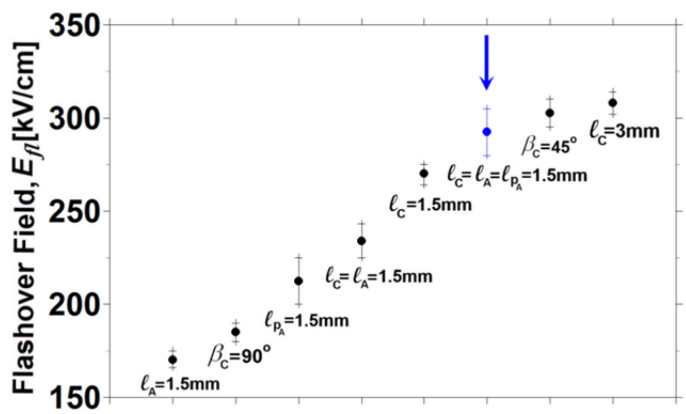

Figure 20. Experimentally measured flashover fields for the geometry of Figure 19 ($l_C = l_A = l_{pA} = 1.5$ mm) (pointed out by blue arrow) compared with results of experiments quoted from Figures 9, 12, 15, and 18.

The geometry of the ATJ shown in Figure 17, which is changed by removing the anode step and adding an anode protrusion, improves the flashover field to a level above that of a geometry with only an $l_C = 1.5$ mm cathode insert, but to a slightly lesser extent than geometries with larger cathode inserts ($l_C = 3$ or 5 mm) (see Figure 9) or that of a simple 45^o inclined insulator.

In Figure 21, the electric field magnitude and the ratio $E_\perp/E_{||}$ along the insulator surface are shown for three cases in Figure 19 with similar and high flashover fields. For all these cases compared in Figure 21a, the electric field approaches zero at the CTJ. An $l_C = 3$ mm cathode insert is sufficient to make the electric field almost the same as that of a 45° inclined insulator along the cathode end half (z = 0 – 5 mm) of the d = 10 mm insulator. For $l_C = l_A = l_{pA} = 1.5$ mm the electric field along the cathode end half is similar to when l_C = 1.5 mm and β_A=90° (see Figure 10a). On the other hand, the electric fields along the insulator surface on the anode end half (z = 5 – 10 mm) and near the ATJ are significantly different for these three cases; however, this seems to have little effect on the value of the flashover field. For a perfect Stygar-type ATJ, the electric field is reduced to zero as compared to infinity for a 45° inclined insulator.

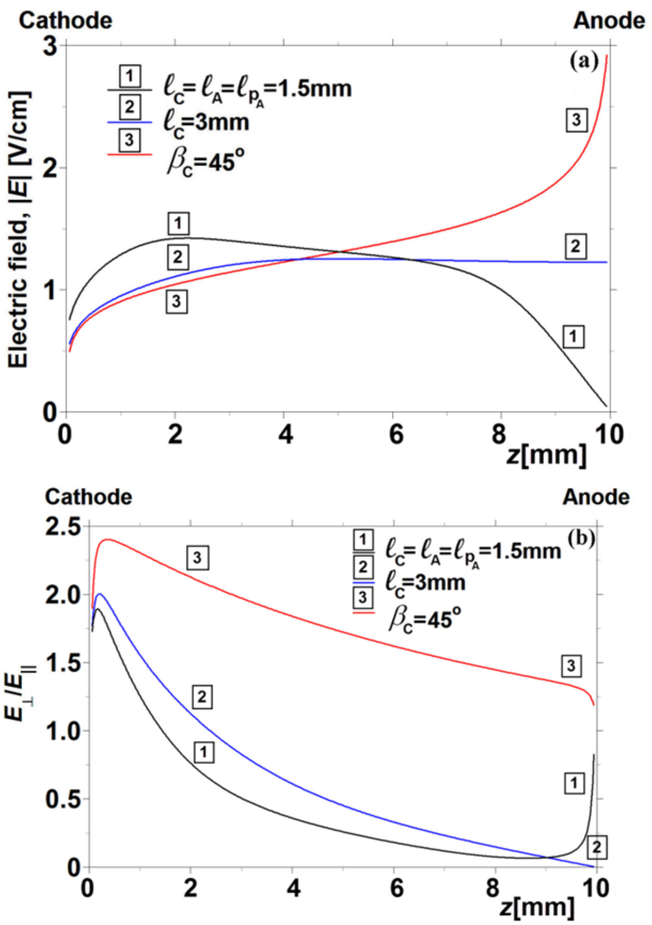

Figure 21. Same as Figure 10 for the geometries of similar flashover fields β_C = 45° (3), $l_C = 3$ mm (2) and $l_C = l_A = l_{pA} = 1.5$ mm (1).

In Figure 21b, the inclination of the electric field along the insulator surface is shown. For all cases, this ratio shows that electrons are deflected away from the insulator surface and that a smaller deflection angle than that for an inclined insulator is sufficient (see also Figures 9-12). As the ATJ is approached, $E_\perp \rightarrow 0$ for $l_C = 3$ mm; for a 45° inclined insulator both $E_\perp$ and $E_\parallel$ approach infinity, whereas for the Stygar-type ATJ both $E_\perp$ and $E_\parallel$ approach zero. Again, these differences and their effect near the ATJ do not seem to strongly affect the experimental value of the flashover field. This result seems to contradict the Stygar et al experimental results [9]. At present, we do not have a sufficiently good explanation for this apparent contradiction. We can only mention that Stygar's experiments were different from those presented here. For instance, in our experiments, when flashover was observed, the insulators tested were not damaged as in Stygar's experiments. In [9], the voltage pulse length was considerably shorter, the samples tested were thicker (40 mm as compared to 10 mm) and the applied voltage respectively much higher, the method used to determine the flashover field did not proceed along a conditioning procedure, and the insulator material was different (Rexolite rather than ULTEM).

4 SUMMARY

We conducted experiments on vacuum surface flashover on insulator surfaces made of ULTEM, having different geometries effected by using cathode and anode inserts and protrusions, by applying HV pulses up to ~300 kV amplitude and µs-scale duration.

The results of these experiments show that the largest value of the flashover fields obtained were in the vicinity of that corresponding to a β_C = 45° inclined insulator and a value equal to this could be obtained by manipulating only the electric fields at and near the CTJ. We confirmed experimentally the conjecture presented in [8] that the orientation of the electric field along the insulator surface is an important factor affecting the flashover field. Indeed, we found that the flashover field increases as primary electrons emitted on conducting surfaces and first generation secondary electrons are more strongly accelerated away from the insulator surface as a result of the inclination of the electric field.

It was also shown that decreasing the value of the electric field at the ATJ has little influence on the flashover process. Even when the electric field decreases to zero as the ATJ is approached, we did not observe a significant increase in the flashover field.

ACKNOWLEDGMENT

The authors are grateful to E. Flyat, K. Gruzinski, S. Gleizer, E. Hillel, A. Baruch and E. Even-Micha for technical assistance in experiments. This work was supported by an RSF (Rafael Science Fund) grant. This fund was established to enhance scientific research collaboration between industry and academic institutions.

We wish to thank the referees for their critical reading of the manuscript and their useful comments.

REFERENCES

[1] H. C. Miller, "Surface flashover of insulators", IEEE Trans. Electr. Insul., Vol. 24, No. 5, pp. 765-786, 1989.

[2] J. C. Martin, A. H. Guenther, M. Kristiansen, *J. C. Martin on Pulsed Power*, Plenum Press, New York, 1996.

[3] S. Humphries, *Principles of Charged Particle Acceleration*, Wiley, New York, Ch. 9.5, 1989.

[4] I. Smith, "The early history of western pulsed power", IEEE Trans. Plasma Sci., Vol. 34, No. 5, pp. 1585-1609, 2006.

[5] M. S. Chung, B.-G. Yoon, P. H. Cutler, and N. M. Miskovsky, "Theoretical Analysis of the Enhanced Electric Field at the Triple Junction", J. Vac. Sci. Technol. B Vol. 22, No. 3, pp. 1240-1243, 2004.

[6] L. Schächter, "Analytic expression for triple-point electron emission from an ideal edge", Appl. Phys. Lett. Vol. 72, No. 4, pp. 421-423, 1998.

[7] M. S. Chung, B.-G. Yoon, P.H. Cutler, N.N. Miskovsky, B.L. Weiss, and A. Mayer, "Configuration-dependent enhancements of electric fields near the quadruple and triple junction", J. Vac. Sci. Technol. B Vol. 28, No. 2, pp. C2A94-C2A97, 2010.

[8] J. G. Leopold, C. Leibovitz, I. Navon and M. Markovits, "Different approach to pulsed high-voltage vacuum-insulation design", Phys. Rev. ST Accel. Beams, Vol. 10, pp. 060401-14, 2007.

[9] W. A. Stygar, J.A. Lott, T. C. Wagoner, V. Anaya, H.C. Harjes, H.C. Ives, Z.R. Wallace, G.R. Mowrer, R.W. Shoup, J.P. Corley, R.A. Anderson, G.E. Vogtlin, M.E. Savage, J.M. Elizondo, B.S. Stoltzfus, D.M. Andercyk, D.L. Fehl, T.F. Jaramillo, D.L. Johnson, D.H. McDaniel, D.A. Muirhead, J.M. Radman, J. J. Ramirez, L. E. Ramirez, R. B. Spielman, K.W. Struve, D. E. Walsh, E. D. Walsh, and M. D. Walsh, "Improved design of a high-vacuum-insulator interface", Phys. Rev. ST Accel. Beams, Vol. 8, pp. 050401-16, 2005, and references therein.

[10] O. Milton, "Pulsed flashover of insulators in vacuum", IEEE Trans. Electr. Insul., Vol. EI-7, No. 1, pp. 9-15, 1972.

[11] A. Watson, "Pulsed flashover in vacuum", J. Appl. Phys., Vol. 38, No. 5, 2019-2023, 1967.

[12] S. P. Bugaev, G. A. Mesyats, "Nanosecond time development of a pulsed discharge at a dielectric-vacuum interface," Sov. Phys. – Tech. Phys., Vol. 10, pp. 930-932, 1966.

[13] S. P. Bugaev, G. A. Mesyats and A. M. Iskoldskii, "Investigation of the pulsed breakdown mechanism at the surface of a dielectric in vacuum," Sov. Phys. – Tech. Phys., Vol. 12, pp. 1358-1369, 1968.

[14] J. G. Leopold, E. Hillel, C. Leibovitz, M. Markovits and I. Navon, "Applying a different approach to pulsed high-voltage insulation", Proc. IEEE Int'l. Power Modulator and High Voltage Conf., Atlanta, GA, USA, pp. 449, 2010,.

[15] J. G. Leopold, U. Dai, Y. Finkelstein, E. Weissman, and S. Humphries, "Optimizing the performance of flat-surface high-gradient vacuum insulators", IEEE Trans. Dielectr. Electr. Insul. Vol. 12, No. 3, pp. 530-536, 2005.

[16] All calculations in the present paper use the FIELD PRECISION XENOS group of codes developed by the S. Humphries. (See: http://www.fieldp.com).